Available online at www.sciencedirect.com
SCIENCE DIRECT®
Journal of Nuclear Materials 323 (2003) 18–28
journal of nuclear materials
www.elsevier.com/locate/jnucmat

Proton irradiation emulation of PWR neutron damage microstructures in solution annealed 304 and cold-worked 316 stainless steels

Bulent H. Sencer [a,*], Gary S. Was [b,1], Mitsuyuki Sagisaka [c,2], Yoshihiro Isobe [c,2], Gillian M. Bond [d,3], Frank A. Garner [e,4]

[a] Department of Nuclear Engineering and Radiological Sciences, The University of Michigan, 2355 Bonisteel, Ann Arbor, MI 48109, USA
[b] Department of Materials Science and Engineering, The University of Michigan, 2355 Bonisteel, Ann Arbor, MI 48109, USA
[c] Nuclear Fuel Industries, Ltd., Noda 950, Kumatori-cho, Sennan-gun, Osaka 590-0491, Japan
[d] Department of Metallurgical and Materials Engineering, New Mexico Institute of Technology, 801 Leroy Place, Socorro, NM 87801, USA
[e] Department of Materials Resources, Pacific Northwest National Laboratory, P.O. Box 999, Battelle Boulevard, P8-15 Richland, WA 99352, USA

Received 7 April 2003; accepted 24 July 2003

Abstract

Solution annealed (SA) 304 and cold-worked (CW) 316 austenitic stainless steels were pre-implanted with helium and were irradiated with protons in order to study the potential effects of helium, irradiation dose, and irradiation temperature on microstructural evolution, especially void swelling, with relevance to the behavior of austenitic core internals in pressurized water reactors (PWRs). These steels were irradiated with 1 MeV protons to doses between 1 and 10 dpa at 300 °C both with or without 15 appm helium pre-implanted at ~100 °C. They were also irradiated at 340 °C, but only after 15 appm helium pre-implantation. Small heterogeneously distributed voids were observed in both alloys irradiated at 300 °C, but only after helium pre-implantation. The pre-implanted steels irradiated at 340 °C exhibited homogenous void formation, suggesting effects of both helium and irradiation temperature on void nucleation. Voids developed sooner in the SA304 alloy than CW316 alloy at 300 and 340 °C, consistent with the behavior observed at higher temperatures (>370 °C) for similar steels irradiated in the EBR-II fast reactor. The development of the Frank loop microstructure was similar in both alloys, and was only marginally affected by pre-implanted helium. Loop densities were insensitive to dose and irradiation temperature, and were decreased by helium; loop sizes increased with dose up to about 5.5 dpa and were not affected by the pre-implanted helium. Comparison with microstructures produced by neutron irradiation suggests that this method of helium pre-implantation and proton irradiation emulates neutron irradiation under PWR conditions.

* Corresponding author. Present address: Materials Science and Technology (MST-8), Los Alamos National Laboratory, P.O. Box 1663, Mailstop G755, Los Alamos, NM 87545, USA. Tel.: +1-505 664 0766; fax: +1-505 667 8021.
E-mail addresses: sencer@lanl.gov (B.H. Sencer), gsw@umich.edu (G.S. Was), sagisaka@nfi.co.jp (M. Sagisaka), gbond@nmt.edu (G.M. Bond), frank.garner@pnl.gov (F.A. Garner).
[1] Tel.: +1-734 763 4675; fax: +1-734 647 7027.
[2] Tel.: +81-724 52 7221; fax: +81-724 52 7225.
[3] Tel.: +1-505 835 5653; fax: +1-505 835 5626.
[4] Tel.: +1-509 376 4136; fax: +1-509 376 0418.

0022-3115/$ - see front matter © 2003 Elsevier B.V. All rights reserved.
doi:10.1016/j.jnucmat.2003.07.007

1. Introduction

Austenitic stainless steels employed as core internal materials in pressurized water reactors (PWRs) have the potential to undergo void swelling under high dose neutron irradiation as they approach their design lifetime of 40 years or extended lifetimes of 60 years [1–5]. However, the amount of swelling data from core internals under PWR irradiation conditions is still rather limited, especially at higher doses [6–12]. Conducting comprehensive neutron irradiations up to a PWR plant life of 40 years, reaching doses ranging from 10 to 100 dpa, and covering relevant parameters such as flux, flux-energy spectrum, temperature, stress, and material parameters would require enormous amounts of time and resources.

Charged particle simulation at accelerated damage rates is often used in such situations in order to forecast the behavior of neutron-irradiated material. The current study uses proton irradiation to study irradiation damage in PWR core internals. For this purpose, the effects of several parameters known to influence microstructure evolution and void swelling were evaluated in this study, focusing on temperature, irradiation dose, helium addition, composition and cold working. The conditions chosen for study were based on the following consideration.

The baffle and former plates of typical PWRs are constructed from annealed AISI 304 stainless steel, and are often bolted with AISI 316, which is usually in the cold-worked (~15%) condition. The surface temperature of these plates is usually near ~300 °C, and the internal temperature of the plates is raised by gamma heating to ~340 °C maximum, although in a few isolated volumes the temperature can approach 400 °C. The dpa rates in PWR internals are on the order of 10^{-7}–10^{-8} dpa/s and can reach maximum exposure levels of ~100 dpa over 40 years.

There is a large amount of swelling data at high neutron exposures for AISI 316 stainless steel from various fast reactors at temperatures above ~365 °C, and a moderate amount of data from mixed spectrum reactors at lower temperatures. For 304 stainless steel, however, there are swelling data at exposures approaching 100 dpa, but only for temperatures above ~380 °C, since all 304 data was generated from structural components of the EBR-II fast reactor, whose inlet temperature was 370 °C.

While helium is generated at rather low rates in fast reactors, it is initially generated at ~1 appm/dpa in 304 and 316 stainless steels in PWR spectra, but accelerates to ~15 appm/dpa after a delay period that is dependent on the local thermal-to-fast neutron ratio [2,6]. Since the proton irradiation procedure used in this study does not allow the helium to be continuously implanted during proton irradiation, 15 appm He was implanted at ~100 °C prior to proton irradiation, a condition that overemphasizes the initial helium influence, but which is a reasonable average helium level over the dose range explored in the study, especially at 5–10 dpa.

2. Experimental procedure

Commercial purity, solution annealed (SA) 304 and 15% cold worked (CW) 316 stainless steel were prepared as bars with dimensions of $25\times4.0\times1.5$ mm. The compositions of the two alloys are summarized in Table 1. Some of the specimens were first implanted with helium at room temperature. Both implantation and proton irradiation were carried out using a tandem accelerator (General Ionex Tandetron) at the University of Michigan Ion Beam Laboratory for Surface Modification and Analysis. Implantation was conducted by hanging the specimen mounted on a metal holder into the helium beam and by successive tilting of the specimen away from the normal in order to spread the implanted helium over a nearly uniform distribution between 1 and 4 μm depth from the surface. The distribution of helium with depth calculated by the Microcal Origin™ computer program is shown in Fig. 1. Unfortunately, helium implantation without full contact with a heat sink leads to some uncertainty in the temperature during implantations. An estimate of the temperature suggests that it was ~100 °C.

The two steels, both with and without 15 appm helium, were then irradiated side-by-side with protons at 300 °C, and also at 340 °C, but only with 15 appm helium pre-injection at this latter temperature. The irradiation was conducted with 1 MeV protons at doses between 1 and 10 dpa at a dose rate of 3.5×10^{-5} dpa/s at the depth of the foil to be examined. As shown in Fig. 2

Table 1
Chemical composition of alloys (wt%)

Alloy type	C	Si	Mn	P	S	Ni	Cr	Mo	Nb	Fe
SA304	0.058	0.51	1.12	0.03	0.004	8.80	18.35	–	–	Balance
CW316	0.039	0.51	1.58	0.028	0.005	12.40	16.80	2.17	0.04	Balance

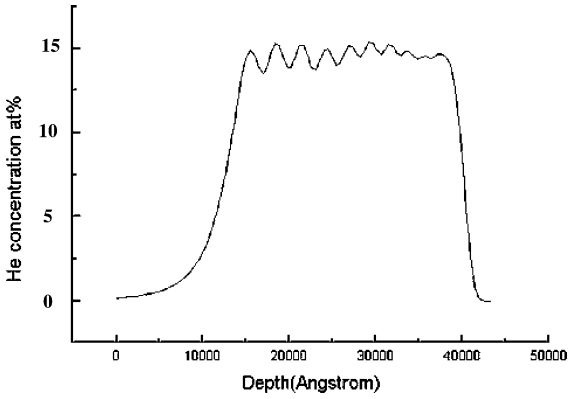

Fig. 1. Implanted helium concentration as a function of depth calculated using Microcal Origin™ program.

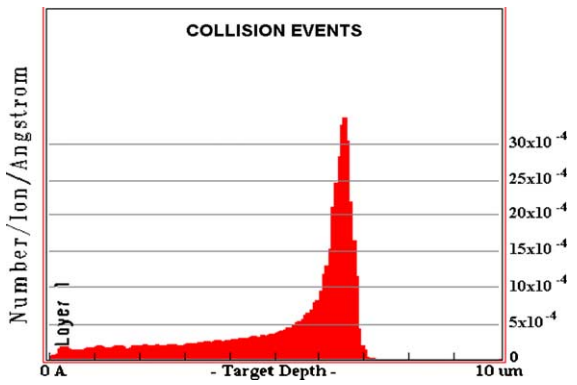

Fig. 2. Calculated 1 MeV proton damage profile TRIM simulation. One mega-electron-volt protons produce a nearly uniform damage profile over the first 4 μm of the proton's range (7 μm).

protons at 1 MeV produce a nearly uniform damage profile over the first 4 μm of the proton's range. The damage profile with depth was calculated by the STRIM 2000™ computer code. It is important to note that the beam was rastered over the specimen surface using a frequency of 255 Hz horizontal by 2062 Hz vertical.

Three TEM disk samples were prepared from the irradiated area of each bar sample as shown in Fig. 3. TEM discs were either punched mechanically or cut using a slurry drill cutter. Subsequently, the discs were electropolished using a single-jet thinner in a 5% perchloric acid and 95% methanol solution at −30 °C with an applied current of 30 mA for 2 s. This procedure removed a layer 3–4 μm deep from the irradiated surface, corresponding to the optimum depth for TEM examination. Beyond 4 μm both the He implantation and the uniform proton irradiation are not maintained. The TEM discs were then back-thinned from the unirradiated side using a 5% perchloric acid and 95%

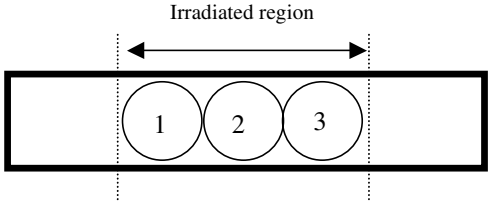

Fig. 3. Configuration of irradiation specimen bars and the location of 3 mm TEM disks to be prepared. The irradiated region is 10 mm in length.

methanol solution at −40 °C with an applied current of 60 mA until perforation.

TEM examinations were conducted with a JEOL 2000E (200 keV) microscope and were directed at Frank loop evolution and void formation. Faulted Frank loops were imaged by the relrod technique and about 400 loops were imaged for each irradiation/material condition to obtain average loop diameters and number densities. If present, voids were imaged using Fresnel contrast and about 400 voids were imaged in each specimen to obtain an average void diameter and number density.

3. Results

Portions of this irradiation study conducted at lower dose levels were published earlier [13] and the final results at all dose levels are presented in this paper. A summary of microstructural characteristics obtained from irradiated specimens of SA304 and CW316 are given in Table 2.

The primary type of dislocation defect that evolved during irradiation was the faulted Frank loop which lies on $\{1\,1\,1\}$ planes with $1/3\langle 1\,1\,1\rangle$ Burgers vector. Frank loops were present at all dpa levels investigated. The loops produced distinctive satellite spots around the fundamental matrix spots in diffraction patterns. These spots are called relrods and are associated with thin planar defects on $\{1\,1\,1\}$ planes. The various satellite spots arise from extended diffraction streaks perpendicular to the four sets of $\{1\,1\,1\}$ planes. An example of a $\langle 1\,1\,0\rangle$ diffraction pattern for a 10 dpa SA304 SS irradiated at 300 °C is shown in Fig. 4. Dark-field images of the loops taken with such streaks reveal the presence of faulted Frank loops. Fig. 5 shows for CW316 an example of the faulted Frank loop images. Their corresponding size distributions are shown in Fig. 6. The loops, although roughly circular, tend to appear elliptical in shape, depending on their orientation in the TEM foil. The relrod technique images Frank loops down to sizes as small as ~1 nm. The use of this technique does not, however, eliminate the possibility that there may be

Table 2
Microstructural parameters of both SA304 and CW316

Alloy	Dose (dpa)	Irradiation temperature (°C)	He pre-injection (appm)	Cavity diameter (nm)	Cavity density ($\times 10^{21}$ m^{-3})	Swelling (%)	Loop diameter (nm)	Loop density ($\times 10^{22}$ m^{-3})	Total dislocation density ($\times 10^{15}$ m^{-2})
SA304	1	300	–	*	*	*	3.71	13.8	1.5
SA304	3.5	300	–	*	*	*	5.58	16.4	2.8
SA304	5.5	300	–	*	*	*	7.06	17.3	3.8
SA304	10	300	–	*	*	*	8.21	19.9	5
SA304	1	300	15	–	–	–	6.6	4.8	1
SA304	2.5	300	15	–	–	–	7.4	7.7	1.8
SA304	3.5	300	15	–	–	–	8.1	5.5	1.4
SA304	10	300	15	–	–	–	9	6.1	1.7
SA304	1	340	15	2.8	10	0.01	7.2	6.7	1.5
SA304	3.5	340	15	4	6	0.02	9	7.2	2
SA304	5.5	340	15	4.1	9	0.03	12.7	4.6	1.8
CW316	1	300	–	*	*	*	4.1	16.6	2.1
CW316	3.5	300	–	*	*	*	5.5	23.0	3.9
CW316	5.5	300	–	*	*	*	8.0	18.1	4.5
CW316	10	300	–	*	*	*	8.6	19.6	5.3
CW316	1	300	15	–	–	–	7.8	4.8	1.2
CW316	2.5	300	15	–	–	–	5.9	1.2	0.2
CW316	3.5	300	15	–	–	–	7.5	11.9	2.8
CW316	10	300	15	–	–	–	8.7	7.2	1.9
CW316	1	340	15	–	–	–	7.4	6.5	1.5
CW316	3.5	340	15	4.3	2.5	0.005	9.6	7	2.1
CW316	5.5	340	15	3.3	4.2	0.005	12.1	6.4	2.4
CW316	10	340	15	4.1	8.9	0.025	12.4	6.6	2.5

(*) No cavities, (–) Heterogeneously distributed patches of voids.

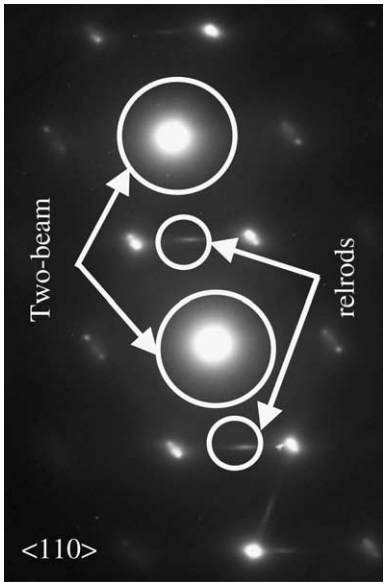

Fig. 4. A diffraction pattern obtained from SA304, 15 appm pre-implanted and irradiated to 10 dpa at 300 °C. The sample was tilted 3–4° off the $\langle 1\,1\,0\rangle$ zone axis to intensify the relrods. Direct beam (0 0 0) and one of $g = \{1\,1\,3\}$ are in a two beam dynamic condition.

dislocation loops smaller than ~1 nm or the possible presence of defect clusters of other types. The relrod technique also does not allow discrimination between extrinsic or intrinsic faults, i.e. faults associated with interstitial or vacancy loops.

The dose dependencies of the average Frank loop size and loop density and in SA304 and CW316 following 1 MeV proton irradiation are shown in Fig. 7. For both cases, with or without 15 appm He pre-implantation, the loop density is saturated at the lowest dose of 1 dpa and then is constant thereafter. The loop size, however, continues to increase over the dose range. There is very little difference between 304 and 316 SS in the dose dependence of loop size or density.

Fig. 7 also shows the effect of helium pre-implantation on loop characteristics at 300 °C for both SA304 and CW316 SS. Samples pre-implanted with 15 appm helium in general show a lower loop density by a factor of about two compared to those without helium pre-implantation. The loop size of pre-implanted samples is correspondingly larger by about 1 nm or ~15% over the unimplanted case. Increasing the temperature from 300 to 340 °C appears to make more of a difference in loop size than in loop density. For 316 SS, the same dependencies were observed, but the difference in loop size

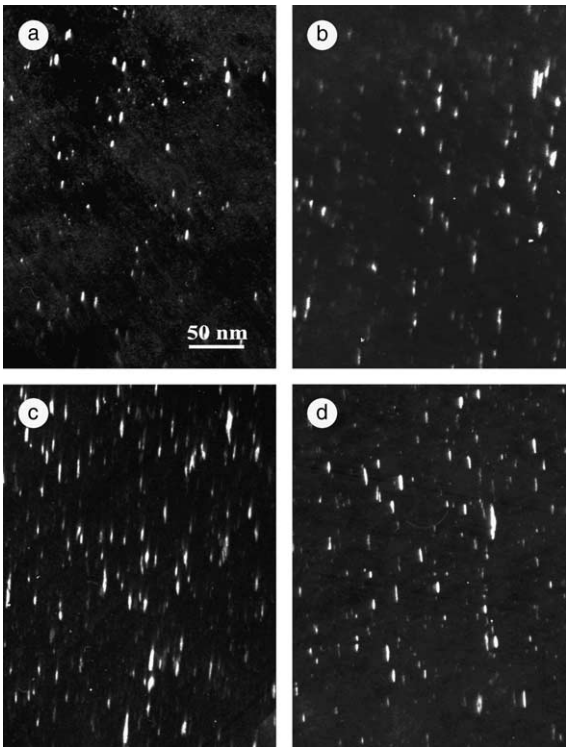

Fig. 5. Dark-field images of the faulted Frank loops in CW316 pre-implanted with 15 appm He and irradiated at 340 °C to (a) 1 dpa, (b) 3.5 dpa, (c) 5 dpa and (d) 10 dpa.

with pre-implanted He is smaller, especially at the maximum dose.

Void formation was investigated using Fresnel contrast, allowing detection of voids down to sizes as small as ~1 nm. Examples of void images at 340 °C in CW316 at a number of dpa levels are shown in Fig. 8 together with void size distributions in Fig. 9. The voids are relatively well-distributed throughout the matrix and swelling increases primarily by an increase in void number density with increasing dose. A similar void behavior was found to occur in SA304. Fig. 10 shows homogeneously distributed voids in SA304 irradiated to 5 dpa at 340 °C and Fig. 11 shows the relative behavior of the void characteristics of the two alloys as the dpa level increases. Void sizes were comparable in both steels, while the void densities and the void swelling is higher in SA304 SS than in CW316, as shown in Fig. 11. Swelling appears to start sooner in SA304 compared to that in CW316.

At 300 °C no voids were found in either alloy in the helium-free condition. In helium pre-implanted specimens, voids averaging ~2 nm were distributed heterogeneously in both alloys. Fig. 12 shows typical examples of isolated heterogeneous voids in both alloys.

4. Discussion

As discussed earlier, although Type 316 stainless steel has been investigated many times in a number of fast and mixed spectrum reactors, the overwhelming majority of high exposure, neutron-induced swelling and microstructural data on Type 304 stainless steel were generated in EBR-II which has an inlet temperature of 370 °C. This steel was used for the structural components of this reactor but was not used in other reactors. Recent studies of the swelling of this steel at PWR-relevant dpa rates obtained from the low-flux reflector and blanket regions of EBR-II indicate that swelling in the range 370–400 °C is significantly accelerated relative to that developing at higher, in-core displacement rates [14,15].

The only significant exception to this 370 °C lower limit on microstructure and swelling data was a report by Brager and Robbins [16] where 304 was observed to develop cavities at 290 °C and ~1 dpa in the ETR mixed spectrum reactor. These cavities behaved more like bubbles than voids, however, both in their distribution and post-irradiation annealing behavior. It was shown by Robbins in a follow-on paper that in ETR the helium generation was ~20 times greater than expected [17], a phenomenon later shown to arise from the previously unknown ^{58}Ni–^{59}Ni two-step helium generation process [18]. Therefore, the cavities observed in the ETR irradiated 304 were dismissed as irrelevant to the void swelling issue.

For the PWR internal structures constructed of annealed 304 plates and cold-worked bolts, it is therefore not possible to predict their relative swelling at PWR-relevant temperatures (300–340 °C) based only on fast reactor experience. In addition, fast reactors such as EBR-II produce very little helium compared to PWRs. If we ignore the helium question for the moment, we know that at temperatures above 370 °C, annealed 304 will always swell sooner and more than cold-worked 316 [19,20]. Similar behavior in comparative swelling was observed by Kiuchi et al. [21] using electron irradiation and Johnston et al. [22] using nickel ion irradiation, both at much higher temperatures of 500 and 625 °C, respectively.

Since the relative behavior of the two steels has been reproduced using both neutrons and charged particles, the authors are confident that proton irradiation can be used to test the extension of this relationship to lower, PWR-relevant temperatures. The results shown in Fig. 11 indeed confirm that at 340 °C annealed 304 swells earlier than cold-worked 316, with a relative delay of ~3.5 dpa, indicating that the trend in relative swelling behavior extends throughout the temperature range of PWR, fast reactor and charged particle interest. The current data also confirm that the difference in swelling arises primarily from differences in void nucleation as

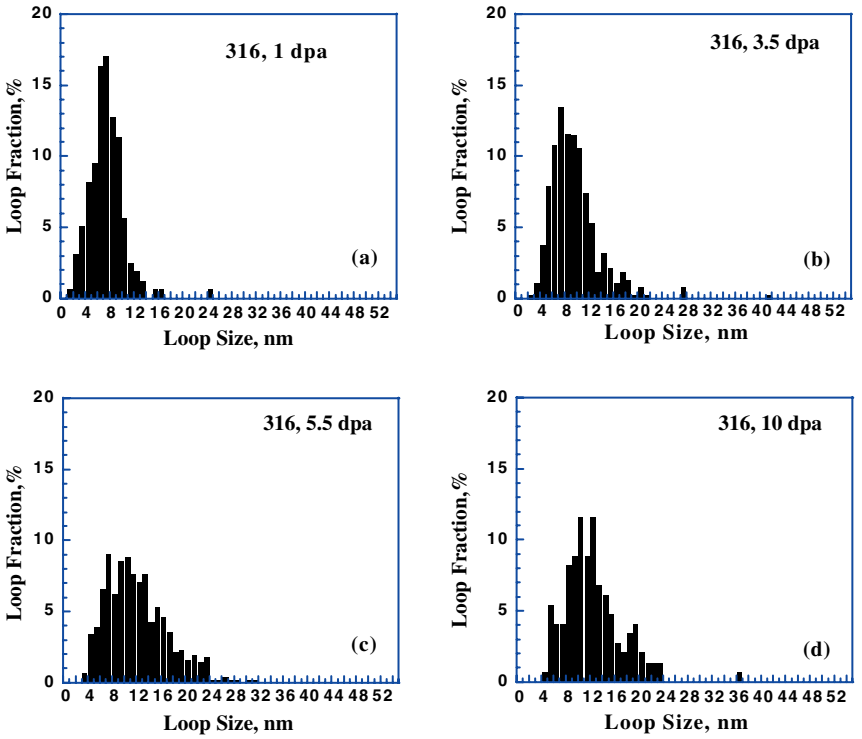

Fig. 6. Loop size distributions in CW316 pre-implanted with 15 appm He and irradiated at 340 °C to (a) 1 dpa, (b) 3.5 dpa, (c) 5.5 dpa and (d) 10 dpa.

opposed to void growth, a very general observation for austenitic steels [23] where the primary effect of all compositional and environmental variables appears to lie only in the incubation or transient regime of swelling.

The data from the current study show that swelling in both steels is much more difficult at 300 °C compared to that at 340 °C, and is essentially impossible without the assistance of helium at the relatively low doses explored in this study. A similar result at 300 °C was observed by Fukuda et al. [24] in both 304 and XM-19. They noted that using 1 MeV protons to 1 dpa did not produce voids unless helium pre-implantation to either 15 or 2000 appm was used. In that case the proton beam was not rastered across the specimen but was held steady. Fukuda et al. [25] also showed in a second paper that voids could be produced at 300, 350 and 400 °C at 1 dpa in both annealed 347 and 310 + Nb using the same proton procedure following 15 appm helium pre-implantation.

Carter et al. irradiated three different heats of Type 304 steel at 400 °C with 3.4 MeV protons in an earlier study conducted at the University of Michigan laboratory without helium pre-implantation, and also observed no voids [26]. This suggests that the helium requirement for swelling resulting from low-dose proton irradiation may extend to temperatures higher than those of PWR interest.

The dpa levels at which void swelling is first observed in both Fukuda's and our study are very low, 1 dpa and perhaps less. The lowest temperature (300 °C) studied is also rather low. Are these low values consistent with neutron data? Garner and coworkers [27–29] have shown that neutron-induced swelling of 300-series austenitic steels indeed extends down to ~300 °C, with no significant swelling below that temperature over a range of dpa levels and dpa rates characteristic of PWR conditions. They have also shown that voids form at very low doses, certainly under several dpa. Therefore, it is not so surprising that voids are found at 300 °C under proton irradiation to 1 dpa. As reported by Edwards et al. [30] neutron irradiation at 275 °C showed no swelling in various heats of 304 and 316 steels. These same heats were irradiated with protons at 360 °C to the same doses to emulate the neutron irradiation, and the results agreed in that there was no evidence of voids in the proton irradiated samples [31]. Similar irradiations in HFIR and ORR have also produced no swelling at 200 °C [32]. Both of these observations tend to confirm that the lower limit of void swelling in austenitic steels is ~300 °C.

Although it is not surprising that helium pre-implantation acts to accelerate void nucleation at these low temperatures where void nucleation appears to be difficult, one should not overlook the fact that the deposited

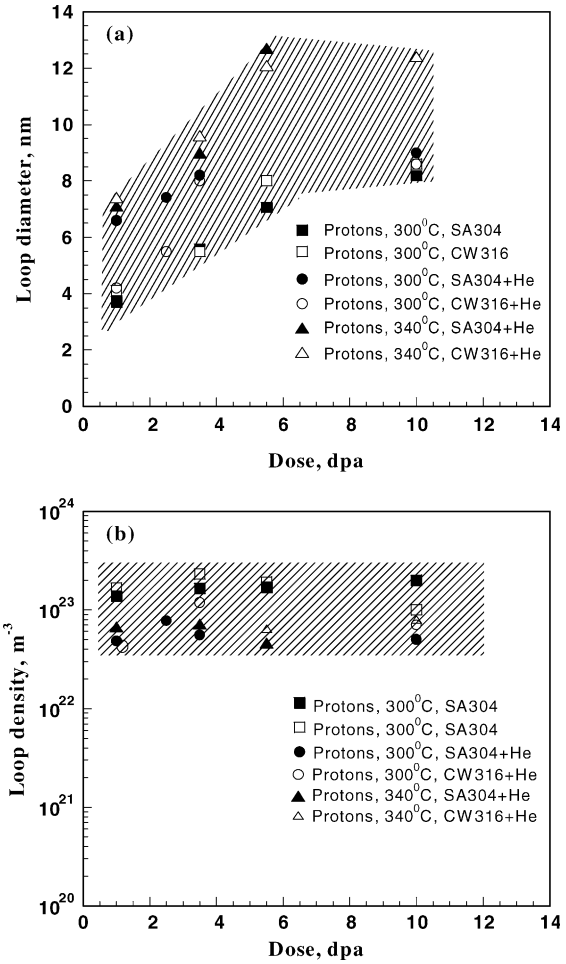

Fig. 7. Compilation of (a) loop diameters and (b) loop densities of SA304 and CW316 irradiated with 1 MeV protons at 300 °C with and without 15 appm He pre-implantation and at 340 °C with 15 appm He pre-implantation.

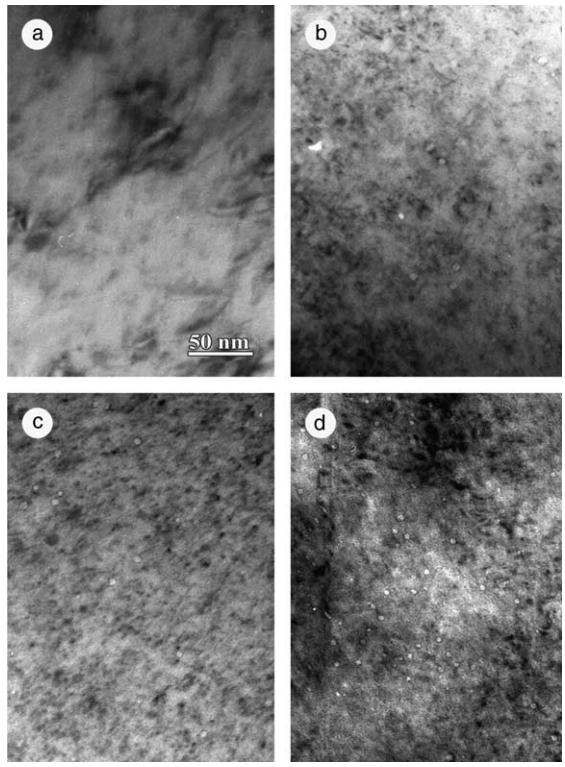

Fig. 8. Bright-field images of voids in CW316 pre-implanted with 15 appm He and irradiated at 340 °C to (a) 1 dpa, (b) 3.5 dpa, (c) 5 dpa and (d) 10 dpa.

protons, acting as hydrogen, are also possibly contributing to void stabilization. Hydrogen is highly mobile and soluble in austenitic steels at 300 °C and it is not generally thought to be strongly bound to vacancy clusters, so trapping with voids is not expected. In fact, there are studies that show that hydrogen deposition and storage is not a prerequisite for void formation. Hudson et al. [33] reported the formation of voids in proton irradiated AISI 321 thin foils at 400 °C in which the protons passed completely through the foil, establishing that hydrogen was not necessary for void formation at this temperature. Tsuchida and Takahashi [34] conducted dual-beam (H^+/electron) in a high voltage electron microscope and reported no enhancement of void nucleation by hydrogen. However Fukuda et al. showed clearly that hydrogen was being stored in the void-containing regions of his proton irradiation experiment [24]. While hydrogen is not necessarily required for void formation, such joint storage of helium and hydrogen might account for the very low dpa levels at which voids are observed in some proton irradiation experiments. Also, it has been suspected that hydrogen absorbed during electrothinning may affect void formation.

Murphy has proposed a model in which hydrogen is trapped in helium–vacancy clusters, leading to enhanced swelling [35]. Other experimental studies have also suggested that hydrogen participates strongly in promoting void nucleation [36–39]. Interestingly, some of the voids found in PWRs at low temperature and low dpa levels have also been attributed to arise from the combined influence of environmental hydrogen and transmutant helium. Garner et al. [40] has recently shown that voids appear to store hydrogen when irradiations proceed in hydrogen-rich environments such as found in PWRs and other water-moderated reactors. In cases where very large amounts of helium and hydrogen were found to be in cavities at 300 °C of 316 type steels [41,42], Garner et al. showed that substantial levels of swelling could be observed, probably due to the combined influence of the two gases to stabilize void nuclei [40]. In the case of a

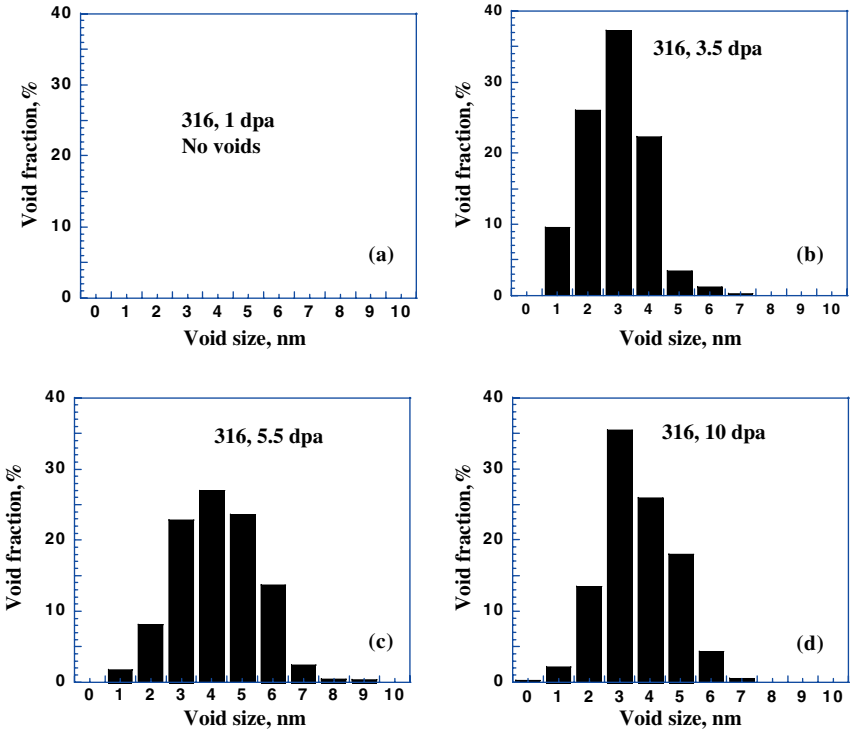

Fig. 9. Void size distributions in CW316 pre-implanted with 15 appm He and irradiated at 340 °C to (a) 1 dpa, (b) 3.5 dpa, (c) 5 dpa and (d) 10 dpa.

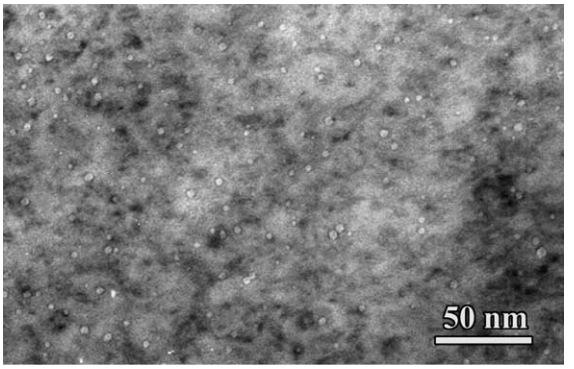

Fig. 10. Bright-field TEM micrograph showing homogeneously distributed voids in SA304 pre-implanted with 15 appm He and irradiated at 340 °C to 5.5 dpa.

PWR baffle bolt examined by Edwards et al., hydrogen was found to be retained in regions of the bolt with significant levels of voids, but not in regions with few or no voids [43].

Fig. 7 shows that the proton-induced loop evolution in the two steels appears at 300 °C to be independent of both cold working and composition. Fig. 13 shows that the neutron-induced loop characteristics are very similar to those of the proton irradiation in the absence of helium, although in this case the comparisons are being made for different heats of steel. However, a similar independence of composition was observed by Edwards et al. [30] in neutron-irradiated 304 and 316 in the annealed condition, irradiated under conditions where the helium generation was relatively low and was produced continuously during irradiation.

At both 300 and 340 °C, however, the Frank loop characteristics were not significantly affected by the 40 °C difference in temperature, but were observed to be partially affected by the pre-implantation of 15 appm helium. The mean size was perhaps increased and the density was decreased with helium addition. It is known that the combined Frank loop and 'black dot' (small loops) population does not change in density from ~150 to ~330 °C in neutron irradiations conducted at rather high helium per dpa ratios [32].

A similar independence of loop microstructure on composition was observed in annealed 304 and 316 by Sencer et al. (following irradiation by 500–800 MeV protons) at much lower temperatures (<100 °C), although in that case the helium and hydrogen retention rates were very much larger [44]. In that high gas environment the loop density was also significantly lower and the loop sizes greater. A similar influence of helium

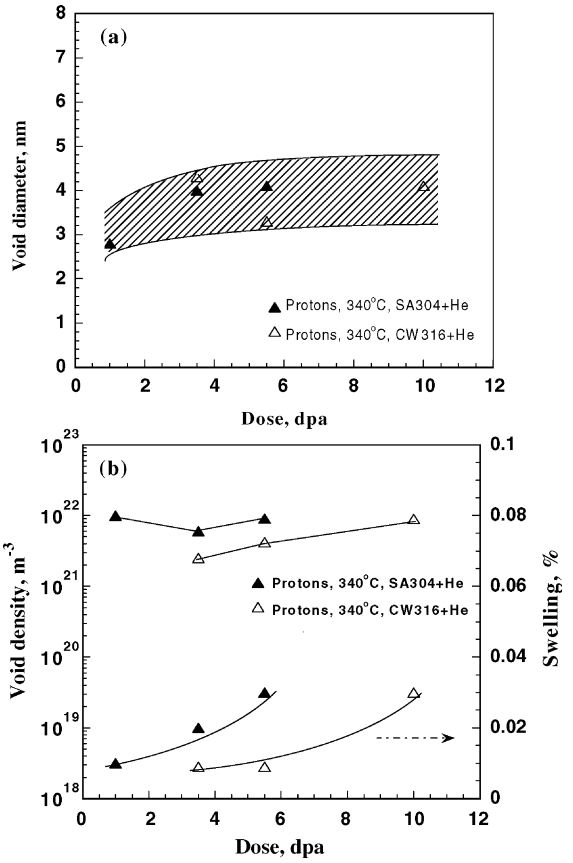

Fig. 11. Compilation of data on proton-induced voids at 340 °C in SA304 and CW316 SS containing 15 appm pre-implanted He.

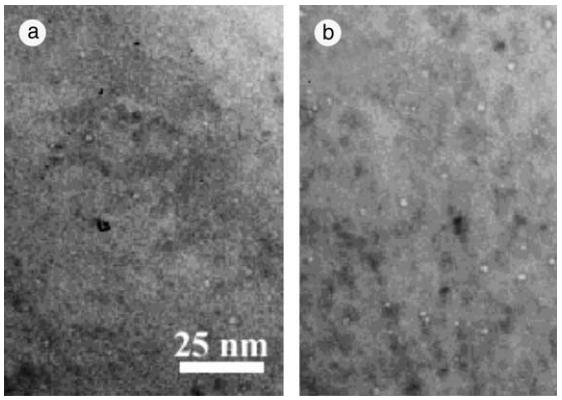

Fig. 12. Bright-field images showing local heterogeneous void distribution observed in 15 appm He pre-implanted (a) CW316 and (b) SA304 after 2.5 dpa irradiation at 300 °C.

to reduce the loop density and increase the size was observed by Kawanishi and Garner in neutron-irradiated Fe–Cr–Ni alloys where differences in helium were

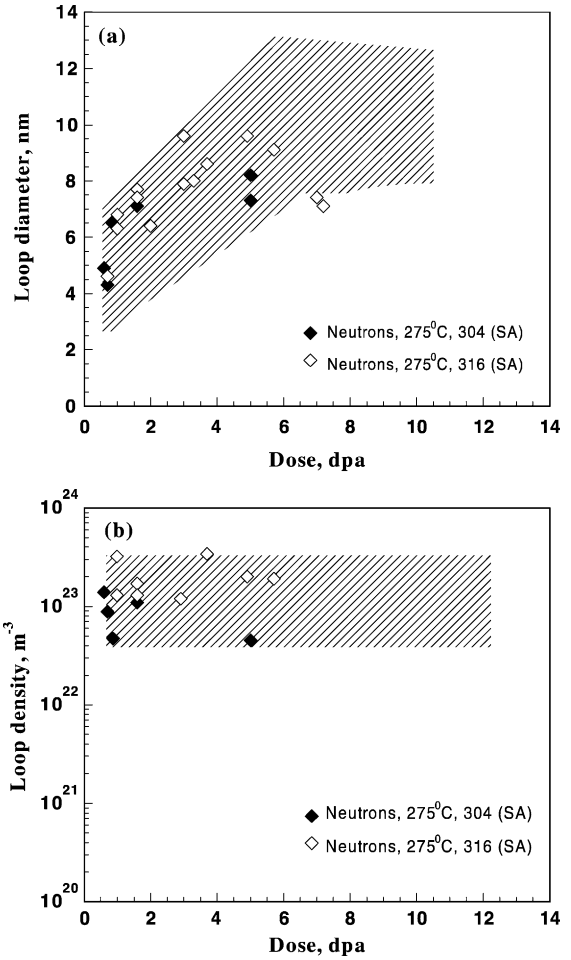

Fig. 13. A comparison of (a) loop diameter and (b) loop density of proton and neutron irradiation of 304 and 316. The irradiation temperature for the neutron study was 275 °C [12]. Shaded regions in graphs show the range of the proton data from Fig. 7.

obtained via isotopic doping and side-by-side irradiation [45].

The influence of helium on loop formation is probably not quite as straightforward as suggested by the above citations, however. There are numerous dual-beam ion irradiation studies of austenitic alloys where the helium per dpa ratio was a variable and in those cases, increasing helium implantation rates led to an increase in loop density, rather than a decrease [46–48]. These studies use co-implantation rather than pre-implantation, and explored rather large levels of helium introduction compared to that of the current study. This was also observed for pre-implantation as noted in a review by Farrell [49].

The different observed effect of helium on loop formation between the current study and the referenced

dual ion studies may be an artifact of the helium injection procedure used in the current studies. Helium pre-injection involves maintaining the specimen in the accelerator for >8 h while injection occurs. The 2.3 MeV helium atoms induce some not-well-defined level of heating in the surface layer, reaching perhaps 100 °C and most likely producing some diffusion or redistribution of carbon, phosphorus and other minor elements that interact with interstitials. The unimplanted specimens did not experience a similar history. In the dual ion irradiation, all specimens at low or high helium co-implantation levels experience the same temperature history but with no pre-seeding with point defects.

In an earlier paper focusing on radiation-induced cracking and its microstructural origins the 'emulation of neutron irradiation effects with protons' was found to be a valid concept [31]. Based on the current and previously published results it appears that at least in the range 275–340 °C and perhaps as low as 100 °C, proton irradiation also simulates the loop-producing and void-inducing characteristics of neutrons. Therefore we conclude that proton irradiation of austenitic steels sufficiently reproduces most aspects of the behavior of neutron irradiation to confidently allow the use of proton simulation to study microstructural evolution under PWR conditions, especially for the lower temperatures characteristic of such irradiations.

5. Conclusions

Both SA304 and CW316 stainless steels were irradiated with 1 MeV protons to doses up to 10 dpa at 300 and 340 °C in order to simulate the relative behavior of these steels during neutron irradiation at comparable temperatures in pressurized water reactors. Based on known neutron-induced trends in both Frank loop populations and void swelling, it appears that the method of proton irradiation described here is a valid simulation of neutron-induced microstructure. Such a simulation requires the pre-introduction of helium to stabilize void nuclei at these temperatures. Hydrogen introduced by the proton irradiation may also play some role in stabilizing void nuclei, but only when helium is present, as no voids form without helium. Under these conditions voids form in these steels at doses as low as 1 dpa at 300–340 °C, and the relative swelling behavior of the two steels mirrors the behavior observed at higher temperatures (>370 °C) in fast reactors.

Acknowledgements

The authors are grateful to V. Rotberg and O. Toader for their help in conducting proton irradiation at the University of Michigan Ion Beam Laboratory. Financial support for B.H. Sencer was provided by the Nuclear Fuel Industries (NFI) of Japan.

References

[1] F.A. Garner, Trans. Am. Nucl. Soc. 71 (1994) 190.
[2] F.A. Garner, L.R. Greenwood, D.L. Harrod, in: Proceedings Sixth International Symposium on Environmental Degradation of Materials in Nuclear Power Systems – Water Reactors, San Diego, CA, 1–5 August 1993, The Minerals, Metals & Materials Society, p. 783.
[3] F.A. Garner, M.B. Toloczko, J. Nucl. Mater. 251 (1997) 252.
[4] F.A. Garner, M.B. Toloczko, S.I. Porollo, A.N. Vorobjev, A.M. Dvoriashin, Yu.V. Konobeev, in: Proceedings Eighth International Symposium on Environmental Degradation of Materials in Nuclear Power Systems – Water Reactors, Amelia Island, Florida, 10–14 August 1997, The Minerals, Metals & Materials Society, p. 839.
[5] F.A. Garner, D.J. Edwards, S.M. Bruemmer, S.I. Porollo, Yu.V. Konobeev, V.S. Neustroev, V.K. Shamardin, A.V. Kozlov, in: International Symposium on Contribution of Materials Investigation to the Resolution of Problems Encountered in Pressurized Water Reactors, Fontevraud, France, 23–27 September 2002, p. 393.
[6] D.J. Edwards, F.A. Garner, B.A. Oliver, S.M. Bruemmer, in: Proceedings of the Tenth International Symposium on Environmental Degradation of Materials in Nuclear Power Systems – Water Reactors, TMS, 2000, in CD format.
[7] L.E. Thomas, S.M. Bruemmer, in: International Symposium on Contribution of Materials Investigation to the Resolution of Problems Encountered in Pressurized Water Reactors, Fontevraud, France, 23–27 September 2002, p. 347.
[8] Goltrant, R. Cauvin, D. Dedydier, A. Trenty, in: International Symposium on Contribution of Materials Investigation to the Resolution of Problems Encountered in Pressurized Water Reactors, Fontevraud, France, 14–18 September 1998, p. 183.
[9] G. Pironet, A. Heuze, O. Goltrant, R. Cauvin, in: International Symposium on Contribution of Materials Investigation to the Resolution of Problems Encountered in Pressurized Water Reactors, Fontevraud, France, 14–18 September 1998, p. 195.
[10] I. Monnet, G.M. Decroix, P. Dubuisson, J. Reuchet, O. Morlent, in: International Symposium on Contribution of Materials Investigation to the Resolution of Problems Encountered in Pressurized Water Reactors, Fontevraud, France, 23–27 September 2002, p. 371.
[11] S.T. Byrne, I. Wilson, R. Shogan, in: International Symposium on Contribution of Materials Investigation to the Resolution of Problems Encountered in Pressurized Water Reactors, Fontevraud, France, 23–27 September 2002, p. 343.
[12] K. Fujii, K. Fukuya, G. Furutani, T. Torimaru, A. Kohyama, Y. Kotah, in: Proceedings of the Tenth International Symposium on Environmental Degradation of Materials in Nuclear Power Systems – Water Reactors, vol. 2, TMS, 2000, in CD format.

[13] M. Sagisaka, T. Fukuda, Y. Isobe, F.A. Garner, B.H. Sencer, G.M. Bond, G.S. Was, T. Kamada, K. Matsueda, in: Proceedings of the Tenth International Symposium on Environmental Degradation of Materials in Nuclear Power Systems – Water Reactors, vol. 2, TMS, 2000, in CD format.
[14] G.M. Bond, B.H. Sencer, F.A. Garner, M.L. Hamilton, T.R. Allen, D.L. Porter, in: 9th International Conference on Environmental Degradation of Materials in Nuclear Power Systems – Water Reactors, 1999, p. 1045.
[15] F.A. Garner, M.L. Hamilton, D.L. Porter, T.R. Allen, T. Tsutsui, M. Nakajima, T. Kido, T. Ishii, J. Nucl. Mater., submitted for publication.
[16] H.R. Brager, R.E. Robbins, Trans. Met. Soc. AIME 242 (1968) 2010.
[17] R.E. Robbins, J. Nucl. Mater. 33 (1969) 101.
[18] L.R. Greenwood, J. Nucl. Mater. 115 (1983) 137.
[19] B.R. Siedel, R.E. Einziger, in: Proceedings of the International Conference on Radiation Effects in Breeder Reactor Materials, AIME, 1977, p. 139.
[20] G.L. Hofman, Nucl. Technol. 47 (1980) 7.
[21] K. Kiuchi, T. Ishiyama, A. Hishinuma, J. Nucl. Mater. 155–157 (1988) 797.
[22] W.G. Johnston, J.H. Rosolowski, A.M. Turkalo, T. Lauritzen, J. Nucl. Mater. 54 (1974) 24.
[23] F.A. Garner, in: Materials Science and Technology: A Comprehensive Treatment, vol. 10A, VCH, 1994, p. 419 (Chapter 6).
[24] T. Fukuda, T. Aoki, Y. Isobe, T. Furuya, A. Hasegawa, K. Abe, J. Nucl. Mater. 258–263 (1998) 1694.
[25] T. Fukuda, M. Sagisaka, Y. Isobe, A. Hasegawa, M. Sato, K. Abe, Y. Nishida, T. Kamada, Y. Kaneshima, J. Nucl. Mater. 2283–2287 (2000) 263.
[26] R.D. Carter, D.L. Damcott, M. Atzmon, G.S. Was, E.A. Kenik, J. Nucl. Mater. 205 (1993) 361.
[27] S.I. Porollo, Yu.V. Konobeev, A.M. Dvoraishin, V.M. Krigan, F.A. Garner, in: 10th International Conference on Environmental Degradation of Materials in Nuclear Power Systems – Water Reactors, 2001, issued on CD format.
[28] V.S. Neustroev, V.K. Shamardin, Z.E. Ostrovsky, A.M. Pecherin, F.A. Garner, in: International Symposium on Contribution of Materials Investigation to the Resolution of Problems Encountered in Pressurized Water Reactors, Fontevraud, France, 14–18 September 1998, p. 261.
[29] F.A. Garner, S.I. Porollo, A.N. Vorobjev, Yu.V. Konobeev, A.M. Dvoriashin, V.M. Krigan, N.I. Budylkin, E.G. Mironova, in: International Symposium on Contribution of Materials Investigation to the Resolution of Problems Encountered in Pressurized Water Reactors, Fontevraud, France, 14–18 September 1998, p. 249.
[30] D.J. Edwards, E.P. Simonen, S.M. Bruemmer, J. Nucl. Mater. 317 (2003) 13.
[31] G.S. Was, J.T. Busby, T. Allen, E.A. Kenik, A. Jenssen, S.M. Bruemmer, J. Gan, A.D. Edwards, P.M. Scott, P.L. Andresen, J. Nucl. Mater. 300 (2002) 198.
[32] M.L. Grossbeck, P.J. Maziasz, A.F. Rowcliffe, J. Nucl. Mater. 191–194 (1992) 808.
[33] J.A. Hudson, R.S. Nelson, R.J. McElroy, J. Nucl. Mater. 65 (1977) 279.
[34] H. Tsuchida, H. Takahashi, J. Nucl. Mater. 239 (1996) 112.
[35] S.M. Murphy, J. Nucl. Mater. 155–157 (1988) 866.
[36] Y. Murase, A. Hasegawa, Y. Yamamoto, J. Nakagawa, H. Shiraishi, J. Nucl. Sci. Techn. 33 (1996) 239.
[37] Y. Murase, Y. Yamamoto, J. Nakagawa, H. Shiraishi, J. Nucl. Mater. 258–263 (1998) 1639.
[38] B. Bullen, G.L. Kulcinski, R.A. Dodd, J. Nucl. Mater. 133&134 (1985) 455.
[39] S. Ohnuki, H. Takahashi, T. Takeyama, F. Wan, J. Nucl. Mater. 133&134 (1988) 459.
[40] F.A. Garner, B.M. Oliver, L.R. Greenwood, D.J. Edwards, S.M. Bruemmer, M.L. Grossbeck, in: 10th International Conference on Environmental Degradation of Materials in Nuclear Power Systems – Water Reactors, 2001, issued on CD format.
[41] M.P. Tanaka, S. Hamada, A. Hishinuma, P.J. Maziasz, J. Nucl. Mater. 155–157 (1988) 801.
[42] S. Hamada, P.J. Maziasz, M.P. Tanaka, M. Suzuki, A. Hishinuma, J. Nucl. Mater. 155–157 (1988) 838.
[43] D.J. Edwards, E.P. Simonen, F.A. Garner, B.A. Oliver, L.R. Greenwood, S.M. Bruemmer, J. Nucl. Mater. 317 (2003) 32.
[44] B.H. Sencer, G.M. Bond, M.L. Hamilton, F.A. Garner, S.A. Maloy, W.F. Sommer, J. Nucl. Mater. 296 (2001) 112.
[45] H. Kawanishi, F.A. Garner, J. Nucl. Mater. 212–215 (1994) 498.
[46] S. Ohnuki, H. Takahashi, R. Nagasaki, J. Nucl. Mater. 155–157 (1988) 823.
[47] Y. Katoh, Y. Kohno, A. Kohyama, J. Nucl. Mater. (1993) 354.
[48] Y. Hidaka, S. Ohnuki, H. Takahashi, S. Watanabe, J. Nucl. Mater. (1993) 330.
[49] K. Farrell, Radiat. Eff. 53 (1980) 175.